Raman imaging of hemozoin within the food vacuole of *Plasmodium falciparum* trophozoites

Bayden R. Wood[a,*], Steven J. Langford[a], Brian M. Cooke[b], Fiona K. Glenister[b], Janelle Lim[a], Don McNaughton[a]

[a] *Centre for Biospectroscopy and School of Chemistry, Monash University, Clayton, Vic. 3800, Australia*
[b] *Department of Microbiology, Monash University, Clayton, Vic. 3800, Australia*

Received 14 July 2003; revised 26 August 2003; accepted 26 August 2003

First published online 6 October 2003

Edited by Felix Wieland

Abstract Micro-Raman spectra of hemozoin encapsulated within the food vacuole of a *Plasmodium falciparum*-infected erythrocyte are presented. The spectrum of hemozoin is identical to the spectrum of β-hematin at all applied excitation wavelengths. The unexpected observation of dramatic band enhancement of A_{1g} modes including ν_4 (1374 cm^{-1}) observed when applying 780 nm excitation enabled Raman imaging of hemozoin in the food vacuole. This unusual enhancement, resulting from excitonic coupling between linked porphyrin moieties in the extended porphyrin array, enables the investigation of hemozoin within its natural environment for the first time.

Key words: Malaria; Raman spectroscopy; Hemozoin; β-Hematin; *Plasmodium falciparum*

1. Introduction

Malaria is responsible for over one million deaths each year with 90% occurring in sub-Saharan Africa [1]. During the intraerythrocytic stage of the life cycle of malaria parasites reactive heme is released upon catabolism of hemoglobin, and is sequestered into a virtually insoluble aggregate known as malaria pigment or hemozoin [2–4]. Heme detoxification by these parasites is critical in preventing reactive free heme damaging biological molecules and disrupting cell membranes [5,6]. Fourier transform infrared spectra indicated an iron–carboxylate bond exists between two hemes in hemozoin and the pigment was spectroscopically identical to the synthetic analogue β-hematin (Fe(III)-protoporphyrin-IX)$_x$ [4]. Electron paramagnetic resonance and Mössbauer spectroscopy determined that both hemozoin and β-hematin have a single $S = 5/2$ iron environment in the bulk phase. Powder diffraction data obtained with synchrotron radiation reported that β-hematin is linked into dimers through reciprocal iron–carboxylate bonds to one of the propionate side chains and the dimers in turn form chains linked by hydrogen bonds [7].

Quinolines such as chloroquine inhibit the formation of hemozoin by binding to heme via the π–π cofacial stacking of planar aromatic structures, resulting in heme-mediated toxicity [8–11]. Free Fe(II) heme is thought to be toxic to the parasite by inducing lipid oxidation [6] and disrupting cell membranes [5] but other explanations have been put forward [9,12]. Studies have shown that many anti-malarial drugs such as chloroquine and its derivatives accumulate in the food vacuole and exert their influence by binding to heme [9]. Direct evidence of drugs binding to heme in vitro is scarce and most of it relies on either measurements of crude trophozoite lysates, chemical methods under non-physiologic conditions or morphologic effects using microscopic techniques. Consequently, the ability to monitor hemozoin within functional erythrocytes and understanding the formation and packing of hemozoin in the food vacuole of the trophozoite has important implications in drug development.

Laser Raman spectroscopy is a powerful technique for elucidating both structural and functional information on heme and other metalloporphyrins [13]. The high symmetry and chromophoric structure of hemes such as hematin (Fe(III)-protoporphyrin-IX-OH) depicted in Fig. 1 results in strong Raman scattering upon excitation with different wavelengths. The strongest enhancement is usually observed when the excitation wavelength lies on (resonance) or near (pre-resonance) an electronic transition. While many studies focus on heme molecules in solution, few studies have investigated hemes within living cells. The first group [14] to report Raman microscopic measurements of single cells demonstrated the sensitivity of the technique to heme moieties in leukocytes, including eosinophil peroxidase and myeloperoxidase [15]. Resonance Raman spectra of normal and *Plasmodium berghei*-infected mouse erythrocytes fixed in methanol were reported using 488 nm excitation [16] and more recently 633 nm excitation [17]. Our work has focussed on characterizing and interpreting the Raman spectra of single functional erythrocytes in both the oxygenated and deoxygenated state [18–20]. In this study micro-Raman spectra of hemozoin within the food vacuole of a *Plasmodium falciparum* trophozoite-infected functional erythrocytes using 488, 514, 568, 633, 780 nm excitation wavelengths are presented. The enhancement of ν_4 (1374 cm^{-1}) at 780 nm enabled Raman imaging of hemozoin within a functional erythrocyte. The unusual Raman enhancement has important implications for the intracellular detection and monitoring of therapeutic agents that are thought to target hemozoin formation.

*Corresponding author. Fax: (61)-3-9905 4597.
E-mail address: bayden.wood@sci.monash.edu.au (B.R. Wood).

0014-5793/03/$22.00
doi:10.1016/S0014-5793(03)00975-X

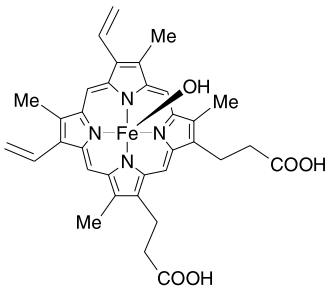

Fig. 1. Schematic representation of hematin, the monomeric precursor of β-hematin.

2. Materials and methods

2.1. Malaria parasites

P. falciparum clone 3D7 [21] was maintained in continuous in vitro culture using human red blood cells suspended in HEPES-buffered RPMI 1640 supplemented with 0.5% AlbumaxII as previously described [22] using standard procedures [23]. Cultures were used for experiments when the majority of parasites were pigmented trophozoites as assessed by examination of Giemsa-stained blood smears.

2.2. Erythrocyte preparation

A 20 μl aliquot of malaria-infected blood was diluted to 10 ml with RPMI 1640 (pH 7.4) at 20°C. The cells were transferred to a 80 mm diameter glass Petri dish previously coated with aluminum by evaporative deposition to produce an 80 nm layer. The Petri dish was further coated with poly-L-lysine and air-dried prior to the addition of the suspension. The cells were allowed to settle (~10 min) before spectra or images were recorded.

2.3. Macromolecules

Hematin was purchased from Sigma-Aldrich. 10 mg of the compound was transferred to a 3 cm aluminum sputter-coated Petri dish containing ~10 ml of phosphate-buffered saline (PBS) at 4°C. The crystals were allowed to settle on the bottom prior to spectral acquisition. Single crystals were targeted with the water immersion objective and the spectra recorded. For each spectrum, 10 scans were accumulated with a 10 s laser exposure time. Preparation of β-hematin was achieved through the methods of Bohle et al. [24] and Egan et al. [25] under standard conditions.

2.4. Raman microscopy

Raman spectra of normal and *P. falciparum*-infected red blood cells were recorded on a Renishaw system 2000 using a 632.8 nm excitation line from a helium–neon laser and 780 nm excitation line generated by a diode laser. The system is equipped with a modified BH2-UMA Olympus optical microscope and a Zeiss ×60 water immersion objective. Spectra were also recorded using the 488 nm and 514 nm excitation lines generated by a Spectra Physics Ar^+ Stabilite 2017 laser system and also a 568 nm excitation line generated by a Spectra Physics Kr^+ Beamlock 2060 laser. In this configuration both lasers were coupled to a Renishaw Raman 2000 spectrometer and interfaced to a Leica Raman microscope using the same water immersion objective as mentioned above. Power at the sample in all cases was 2 ± 0.1 mW for a 1–2 μm laser spot size. Spectra were recorded between 1800 and 200 cm^{-1} with a resolution of ~1–2 cm^{-1}. For each spectrum five scans were accumulated and the laser exposure for each scan was 10 s. The laser exposure was interrupted between scans while the grating repositioned to its starting position because constant exposure resulted in hemolysis and photodissociation.

2.5. Raman imaging

Raman images of malaria-infected erythrocytes were generated at the late trophozoite stage using the 780 nm diode laser with a 120 s laser exposure time. The image was collected by first calibrating the position of ν_4 (1374 cm^{-1}) by recording a filter spectrum of the hemozoin over the 1800–200 cm^{-1} range. Images were recorded by defocussing the laser approximately 15% to encapsulate the cell and the scattered light was transmitted through a polarizer. A background image was also recorded at 1800 cm^{-1}, well away from all other bands, and this image was subtracted from the ν_4 image to minimize the effects of fluorescence and to remove inconsistencies within the laser spot.

3. Results

Raman spectra of hemoglobin and hemozoin in a *P. falciparum*-infected erythrocyte along with a spectrum of synthesized β-hematin using 632.8 nm excitation are shown in Fig. 2. The spectra of hemozoin and hemoglobin were recorded from the same cell in RPMI 1640. The spectrum of β-hematin, synthesized using several methods including a modified protocol developed by Bohle et al. [2], was also recorded in PBS and is essentially identical to the spectrum of hemozoin within the cell, confirming the identical structure of these compounds within functional erythrocytes. The spectrum is very similar to the spectrum recorded by Bohle et al. [2] of β-hematin using 647 nm excitation. Bands in the spectra of hemozoin and hemoglobin at 632.8 nm mainly arise from porphyrin vibrations with little or no contribution from protein, lipid, carbohydrate and other macromolecules [18]. The spectrum of hemozoin exhibits little interference from hemoglobin due to the high concentration (20 mM) and the unusual band enhancement that characterizes the aggregated complex at long excitation wavelengths. Bands in the 1650–1550 cm^{-1} region of hemoglobin are assigned to porphyrin C–C and C=C vibrations, when the Fe atom is in the low spin oxygenated state [18]. Conversely hemozoin exhibits a band profile consistent with a 5-coordinate high spin ($S = 5/2$) heme complex with strong bands at 1623, 1587, 1569 and 1551 cm^{-1} which have been previously assigned [26]. Bands between 1400 and 1300 cm^{-1} are mainly associated with pyrrole in-phase breathing vibrations with different phasing [27], the intensity of which varies between hemoglobin and hemozoin. Bands at 1239 and 1220 cm^{-1} assigned to C–H methine vibrations of the porphyrin [27] appear at 1248 and 1224 cm^{-1} in hemoglobin. It is interesting to note the dramatic intensity of the low wavenumber bands appearing at 402, 374, 344, 315 cm^{-1}. These bands also appear in hematin but are much less enhanced and slightly shifted. The bands are therefore assigned to Fe–N stretching vibrations of the porphyrin moieties based on their low wavenumber values and presence in all three compounds. The band at 514 cm^{-1} has been tentatively assigned to the Fe–O stretching vibration based on its absence in hemin [2].

Fig. 3 depicts Raman spectra of hemozoin within intact parasitized red blood cells for 488, 514, 568, 633 and 780 nm excitation lines. Transmittance UV-visible spectrum of β-hematin measured as a potassium bromide pellet shows the Soret band at 406 and Q bands at 510, 538, 580 and 644 nm [2]. No major electronic transition is observed at 780 nm, yet the most dramatic band enhancement, relative to the normalization band ν_{10} (1623 cm^{-1}), occurs at this wavelength. In particular, bands characteristic of totally symmetric A_{1g} modes including 1570, 1371, 795, 677 (ν_6) and 344 cm^{-1}, along with bands at 1552, 1220 and 755 cm^{-1} associated with B_{1g} modes, have become dramatically enhanced. Bands in the 850–600 cm^{-1} region, which include out-of-plane modes and iron- ligand modes, are also enhanced compared to the shorter excitation wavelengths. Raman spectra of hemoglobin within the erythrocyte at 780 nm exhibit poor signal-to-noise with a broad shape baseline indicative of fluorescence.

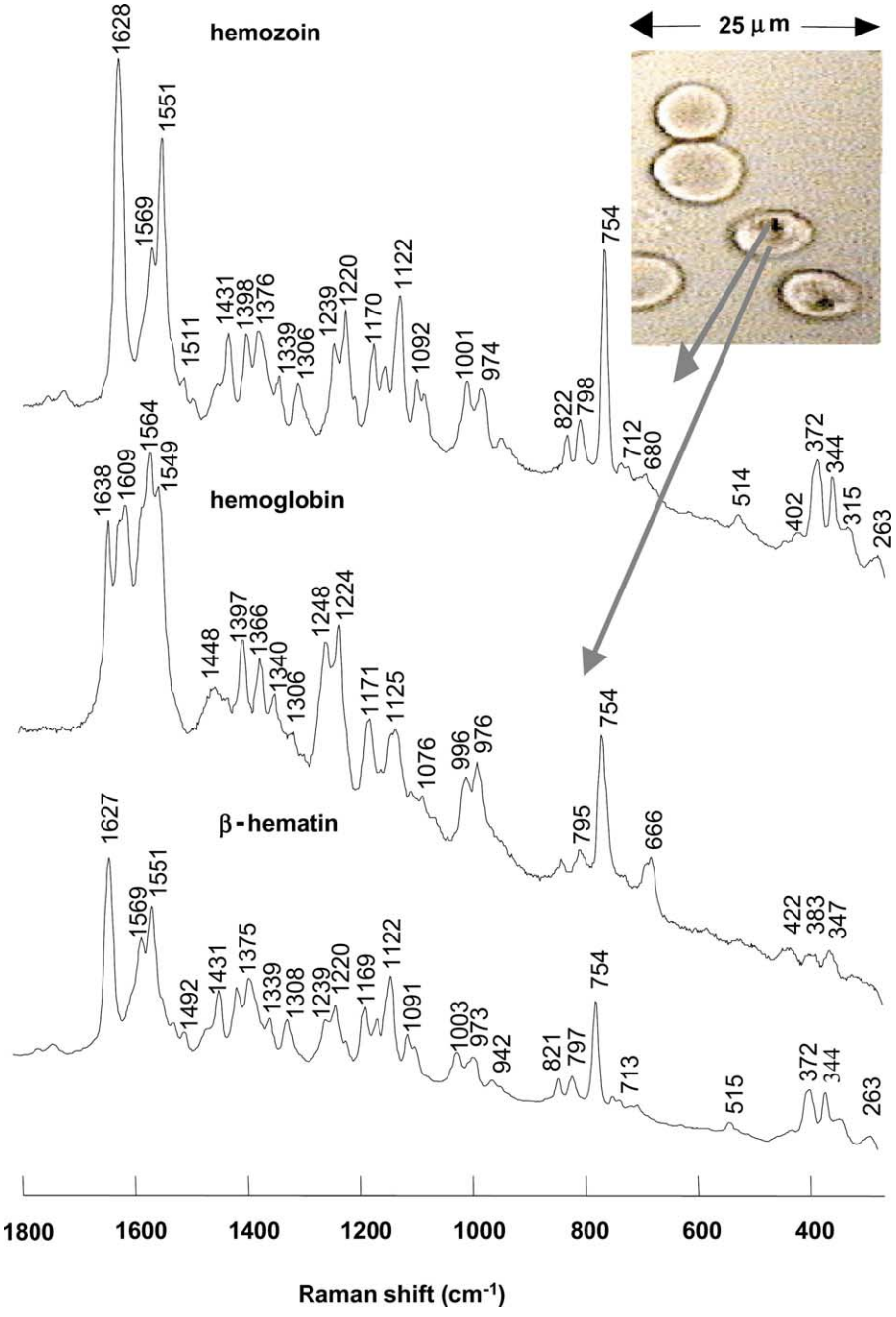

Fig. 2. Photomicrograph of *P. falciparum*-infected erythrocytes (late trophozoite stage) showing the food vacuoles containing hemozoin. The arrows indicate the laser targets namely the food vacuole and the surrounding hemoglobin. The corresponding spectra are compared with synthesized β-hematin.

Fig. 4 shows a photomicrograph of malaria-infected cell in the late trophozoite phase and the corresponding 780 nm excitation Raman image of the 1374 cm^{-1} band showing the food vacuole containing hemozoin. Due to the long excitation wavelength and defocussed laser beam the cell does not lyse during this exposure. The Raman spectra of β-hematin and hematin are also compared with the spectrum of hemozoin from the imaged cell. The spectra of hemozoin and β-hematin are essentially identical at this wavelength. The spectrum of hematin differs from the dimeric analogues mainly in terms of band enhancement. In particular bands at 1571, 1376, 1241–1240, 974, 944, 821, 796, 710, 678 cm^{-1} are dramatically enhanced in hemozoin and β-hematin compared to hematin.

4. Discussion

The unusual enhancement from hemozoin, in combination with the poor enhancement of hemoglobin at 780 nm, enables Raman imaging of the pigment within the trophozoite. It is suggested the extraordinary band enhancement observed in hemozoin compared to hematin results from excitonic coupling between porphyrin moieties in the extended array. The exciton model is based on the quantum mechanical precept

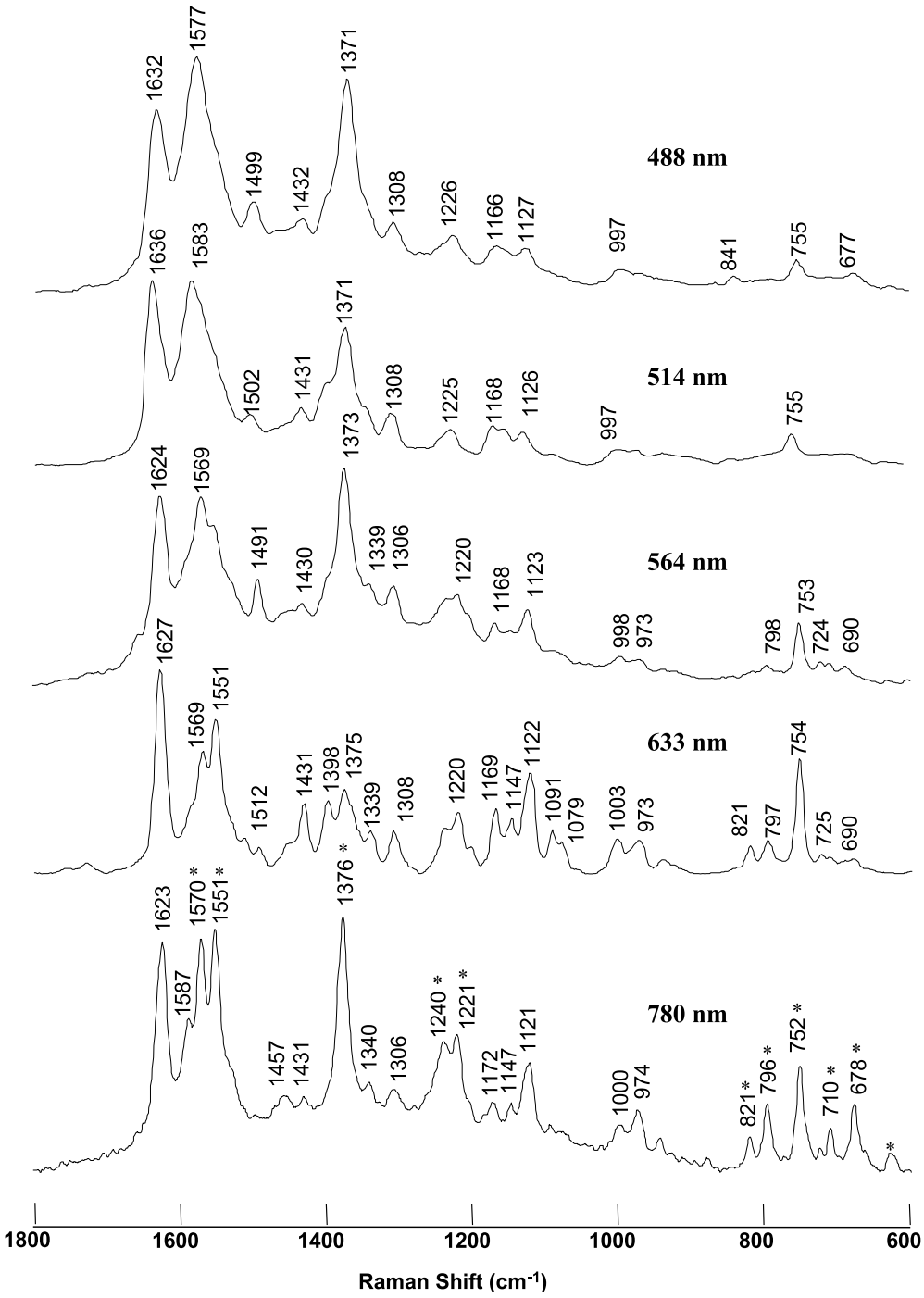

Fig. 3. Micro-Raman spectra recorded of hemozoin within the food vacuoles of *P. falciparum* trophozoites at different excitation wavelengths. The asterisks highlight bands in the 780 nm spectrum that appear dramatically enhanced relative to ν_{10} (1623 cm^{-1}) compared to the other wavelengths investigated.

that electronic energy is distributed throughout the aggregate [28]. This arises because interactions between induced transition dipole moments form a superposition of states resulting in an electronic band of states that enables the movement of electrons throughout the aggregate [28]. Akins et al. [28] demonstrated that the enhancement of Raman scattering is concomitant with the formation of aggregates for a variety of *N*-protonated porphyrins [29–31]. They advanced the theory of aggregated enhanced Raman scattering by incorporating molecular excitonic concepts in a quantum theory analytical expression for aggregated molecules. The enhancement of vibrational modes can be explained in terms of an increase-size effect and near-resonance terms in the polarizability [28]. Excitonic coupling will essentially split the electronic states into a broad band of states with different geometries, energies, and oscillator strengths. The Raman intensities for a particular wavelength will then reflect the extent of the excitonic coupling [19]. The hemozoin and β-hematin porphyrin array enables delocalized electrons to migrate between porphyrins via the propionate linkage. The polarizability ellipsoid of the he-

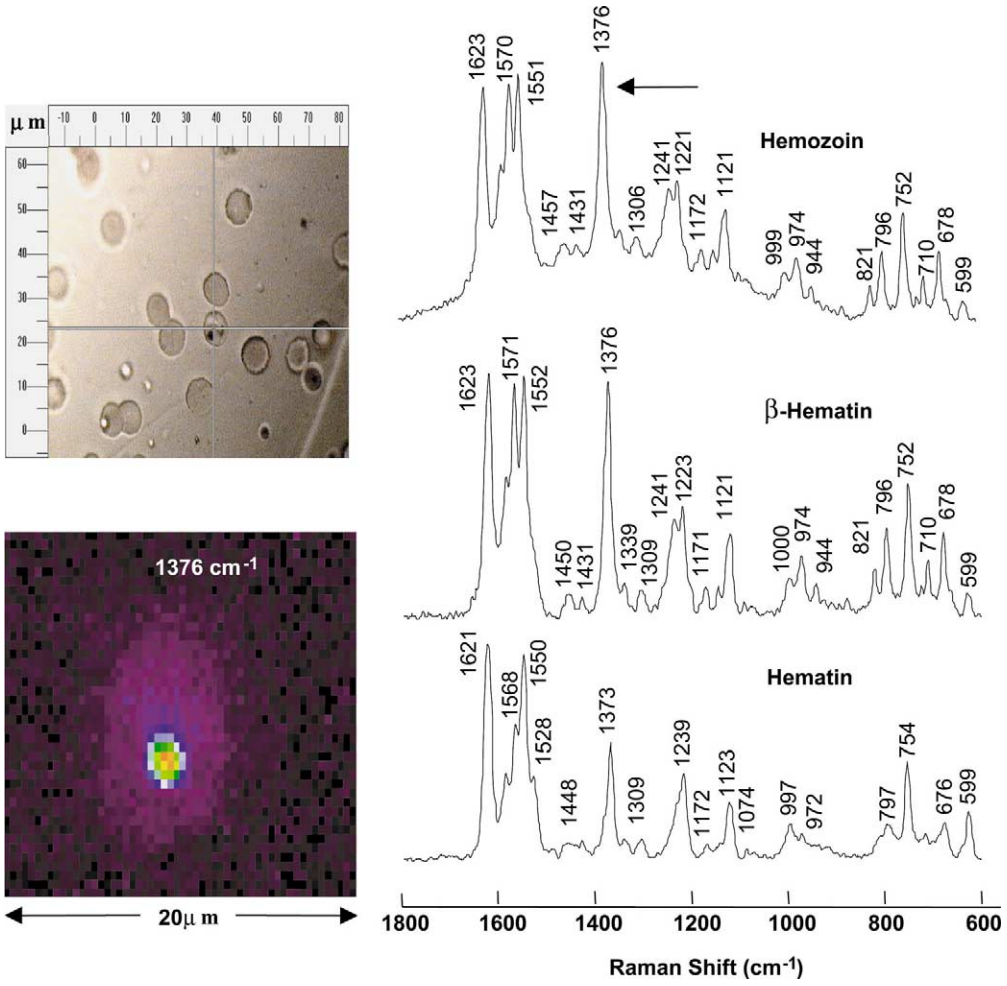

Fig. 4. Photomicrograph and corresponding Raman image of the 1374 cm^{-1} band clearly showing the parasite's food vacuole along with spectra of hemozoin, β-hematin and hematin all acquired using 780 nm excitation. The arrow highlights the totally symmetric mode ν_4 at 1374 cm^{-1}.

mozoin and β-hematin arrays would be much larger than monomeric hematin, consequently the magnitude of the Raman scattering for normal modes would be enhanced. In an extended array, where the porphyrin multimers are linked together by hydrogen bonds to form chains, the polarizability ellipsoid could conceivably extend the length of chain. The oscillatory field necessary to induce a dipole moment in this extended array may require long excitation wavelengths thus providing a plausible explanation for the extraordinary enhancement observed at 780 nm.

The formation of hemozoin appears to prevent heme toxicity to the parasite and is thought to be the primary target for quinoline and non-iron porphyrin drugs [32]. The quinolines are thought to 'cap' hemozoin formation by binding to the heme through π–π stacking of the aromatic structures [9]. Other anti-malarials that accumulate in the food vacuole include the artemisinins, aryl-alcohol anti-malarials, and the anti-malarial peroxides, which are thought to exert their activity through the interaction with heme [9]. Such heme–drug interactions could conceivably be monitored in the functional red blood cell with this approach, either directly by detecting Raman scattering from the drug in the food vacuole, or indirectly by observing changes in the relative intensity of the hemozoin bands. In the latter case such enhancement differences may reflect a reduction in excitonic coupling if the drug of interest indeed 'caps' the formation of hemozoin. Studies investigating the action of chloroquine on hemozoin formation in vitro are currently under way in our laboratory.

Acknowledgements: This work is supported by an Australian Research Council Large Grant (DP0450573). B.M.C. is supported by the National Health and Medical Research Council of Australia and is the recipient of grants from the National Institute of Health (NIH, Grants DK32094-10 and A144008-04A1). We thank Prof. Robert Armstrong and Dr. Elizabeth Carter (School of Chemistry, University of Sydney) for use of the Spectra Physics Ar^+ Stabilite 2017 and Spectra Physics Kr^+ Beamlock 2060 laser systems. We also thank Mr. Finlay Shanks (Monash University) for instrument support and maintenance.

References

[1] Greenwood, B. and Mutabingwa, T. (2002) Nature 415, 670–672.
[2] Bohle, D.S., Conklin, B.J., Cox, D., Madsen, S.K., Paulson, S., Stephens, P.W. and Yee, G.T. (1994) Am. Chem. Soc. Symp. Ser. 572, 497–515.
[3] Francis, S., Sullivan, D.J. and Goldberg, D. (1997) Annu. Rev. Micobiol. 51, 97–123.
[4] Slater, A.F.G., Swiggard, W.J., Orton, B.R., Flitter, W.D., Goldberg, D., Cerami, A. and Henderson, G.B. (1991) Proc. Natl. Acad. Sci. USA 88, 325–329.

[5] Schmitt, T.H., Frezzatti, W.A.J. and Scheier, S. (1993) Arch. Biochem. Biophys. 307, 96–103.
[6] Sugioka, Y. and Suzuki, M. (1991) Biochim. Biophys. Acta 1074, 19–24.
[7] Pagola, S., Stephens, P.W., Bohle, D.S., Kosar, A.D. and Madsen, S.K. (2000) Nature 404, 307–310.
[8] Egan, T.J. and Marques, H.M. (1999) Coord. Chem. Rev. 192, 493–517.
[9] Ridley, R.G. (2002) Nature 415, 686–693.
[10] Ridley, R.G., Dorn, A., Vippagunta, S.R. and Vennerstrom, J.L. (1997) Ann. Trop. Med. Parasitol. 91, 559–566.
[11] Vippagunta, S.R., Dorn, A., Matile, H., Bhattacharjee, A.K., Karle, J.M., Ellis, W.Y., Ridley, R.G. and Vennerstrom, J.L. (1999) J. Med. Chem. 42, 4630–4639.
[12] Ginsburg, H. and Krugliak, M. (1999) Drug Resist. Update 2, 63–70.
[13] Spiro, T.G. and Li, X.-Y. (1988) in: Biological Applications of Raman Spectroscopy, Vol. 3 (Spiro, T.G., Ed.), pp. 1–38, Wiley, New York.
[14] Puppels, G.J., de Mul, F.F.M., Otto, C., Greve, J., Robert-Nicoud, M., Arndt-Jovin, D.J. and Jovin, T.M. (1990) Nature 347, 301–303.
[15] Puppels, G.J., Garritsen, G.M.J., Segers-Nolten, G.M.J., De Mul, F.F.M. and Greve, J. (1991) Biophys. J. 60, 436–446.
[16] Ong, C.W., Shen, Z.X., Ang, K.K.H., Kara, U.A.K. and Tang, S.H. (1999) Appl. Spectrosc. 53, 1097–1101.
[17] Ong, C.W., Shen, Z.X., Ang, K.K.H., Kara, U.A.K. and Tang, J. (2002) Appl. Spectrosc. 56, 1126–1131.
[18] Wood, B.R., Tait, B. and McNaughton, D. (2001) Biochim. Biophys. Acta 1539, 58–70.
[19] Wood, B.R. and McNaughton, D. (2002) J. Raman Spectrosc. 33, 517–523.
[20] Wood, B.R. and McNaughton, D. (2002) Biopolymers (Biospectroscopy) 67, 259–262.
[21] Walliker, D. et al. (1987) Science 236, 1661–1666.
[22] Cranmer, S.L., Magowan, C., Liang, J., Coppel, R.L. and Cooke, B.M. (1997) Trans. R. Soc. Trop. Med. Hyg. 91, 363–365.
[23] Trager, W. (1994) Methods Cell Biol. 45, 7–26.
[24] Bohle, D.S. and Helms, J.B. (1993) Biochem. Biophys. Res. Commun. 193, 504–508.
[25] Egan, T.J., Ross, D.C. and Adams, P.A. (1994) FEBS Lett. 352, 54–57.
[26] Brémard, C., Kowalewski, P. and Merlin, J.C. (1992) J. Raman Spectrosc. 23, 325–333.
[27] Hu, S., Smith, K.M. and Spiro, T.G. (1996) J. Am. Chem. Soc. 118, 12638–12646.
[28] Akins, D.L., Özcelik, S., Zhu, H.-R. and Guo, C. (1997) J. Phys. Chem. 101, 3251–3259.
[29] Akins, D.L., Zhu, H.-R. and Guo, C. (1994) J. Phys. Chem. 98, 3612–3618.
[30] Akins, D.L., Özcelik, S., Zhu, H.-R. and Guo, C. (1996) J. Phys. Chem. 100, 14390–14396.
[31] Akins, D.L., Zhu, H.-R. and Guo, C. (1996) J. Phys. Chem. 100, 5420–5425.
[32] Monti, D., Vodopivec, B., Basilico, N., Olliaro, P. and Taramelli, D. (1999) Biochemistry 38, 8858–8863.